Understanding Energy-Level Alignment in Donor–Acceptor/Metal Interfaces from Core-Level Shifts

Afaf El-Sayed,[†,▲] Patrizia Borghetti,[‡,§,▲] Elizabeth Goiri,[‡,▲] Celia Rogero,[‡,§] Luca Floreano,[⊥] Giacomo Lovat,[⊥] Duncan John Mowbray,[‡,∥] Jose Luis Cabellos,[‡,∥] Yutaka Wakayama,[¶] Angel Rubio,[‡,§,∥] Jose Enrique Ortega,[†,‡,§,*] and Dimas G. de Oteyza[§,#,*]

[†]Departamento Fisica Aplicada I, Universidad del Pais Vasco UPV/EHU, E-20018 San Sebastian, Spain, [‡]Donostia International Physics Center, Paseo Manuel Lardizabal 4, E-20018 San Sebastian, Spain, [§]Centro de Fisica de Materiales CSIC/UPV-EHU-Materials Physics Center, E-20018 San Sebastian, Spain, [⊥]CNR-IOM, Laboratorio Nazionale TASC, Basovizza SS-14 Km. 163.5, I-34149, Trieste, Italy, [∥]Nano-Bio Spectroscopy Group and ETSF Scientific Development Center, Departamento de Fisica de Materiales, Universidad del Pais Vasco UPV/EHU, Avenida de Tolosa 7, E-20018 San Sebastian, Spain, [¶]International Center for Materials Nanoarchitectonics (WPI-MANA), National Institute for Materials Science, 1-1 Namiki, Tsukuba 305-0044, Japan, and [#]Department of Physics, University of California, Berkeley, California 94720, United States. [▲]These authors contributed equally.

ABSTRACT The molecule/metal interface is the key element in charge injection devices. It can be generally defined by a monolayer-thick blend of donor and/or acceptor molecules in contact with a metal surface. Energy barriers for electron and hole injection are determined by the offset from HOMO (highest occupied) and LUMO (lowest unoccupied) molecular levels of this contact layer with respect to the Fermi level of the metal electrode. However, the HOMO and LUMO alignment is not easy to elucidate in complex multicomponent, molecule/metal systems. We demonstrate that core-level photoemission from donor–acceptor/metal interfaces can be used to straightforwardly and transparently assess molecular-level alignment. Systematic experiments in a variety of systems show characteristic binding energy shifts in core levels as a function of molecular donor/acceptor ratio, irrespective of the molecule or the metal. Such shifts reveal how the level alignment at the molecule/metal interface varies as a function of the donor–acceptor stoichiometry in the contact blend.

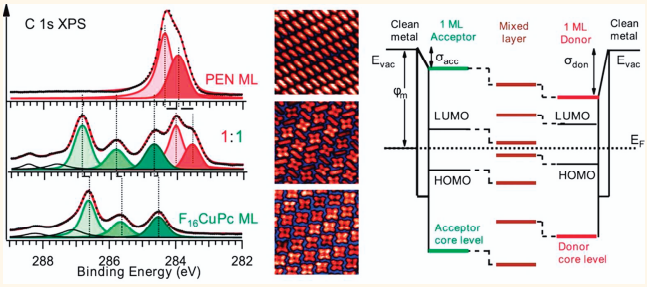

KEYWORDS: metal–organic interfaces · energy-level alignment · Fermi-level pinning · vacuum-level pinning · XPS · molecular blends

Donor–acceptor/metal interfaces are of utmost importance in organic optoelectronics applications such as solar cells.[1−3] Much insight into interface properties can be gained by studying simple donor–acceptor/metal architectures, such as two-dimensional (2D) donor–acceptor networks, which, for example, may segregate from multilayers or blends and form the stable phase in direct contact with the metal.[4] In this work, we use planar aromatic molecules with conjugated π planes because they possess the appropriate morphology to investigate molecule–molecule and molecule/surface electronic interactions in 2D donor–acceptor/metal systems.[5−7] An important question that arises is how such interactions affect the molecular electronic level alignment; that is, how do the highest occupied molecular orbital, HOMO, and the lowest unoccupied molecular orbital, LUMO, align with respect to the metal Fermi energy for a donor–acceptor blend? Two radically distinct scenarios are generally considered, which depend on the way molecules interact with the metal electrode.[8,9] For relatively strong molecule/surface interactions, one expects chemisorption and a high density of interface states which pin the molecular levels to the metal Fermi energy. One good example is that of perylene tetracarboxylic dianhydride (PTCDA) on metal surfaces.[10,11] However, if molecule/surface interactions are weak, the molecular levels might be pinned to the vacuum level of the system, like in condensed noble gases.[12] This is important for devices based on donor–acceptor blends since vacuum-level changes may arise from changes in the donor–acceptor

* Address correspondence to enrique.ortega@ehu.es, d_g_oteyza@ehu.es.

Received for review April 25, 2013 and accepted July 24, 2013.

Published online July 24, 2013
10.1021/nn4020888

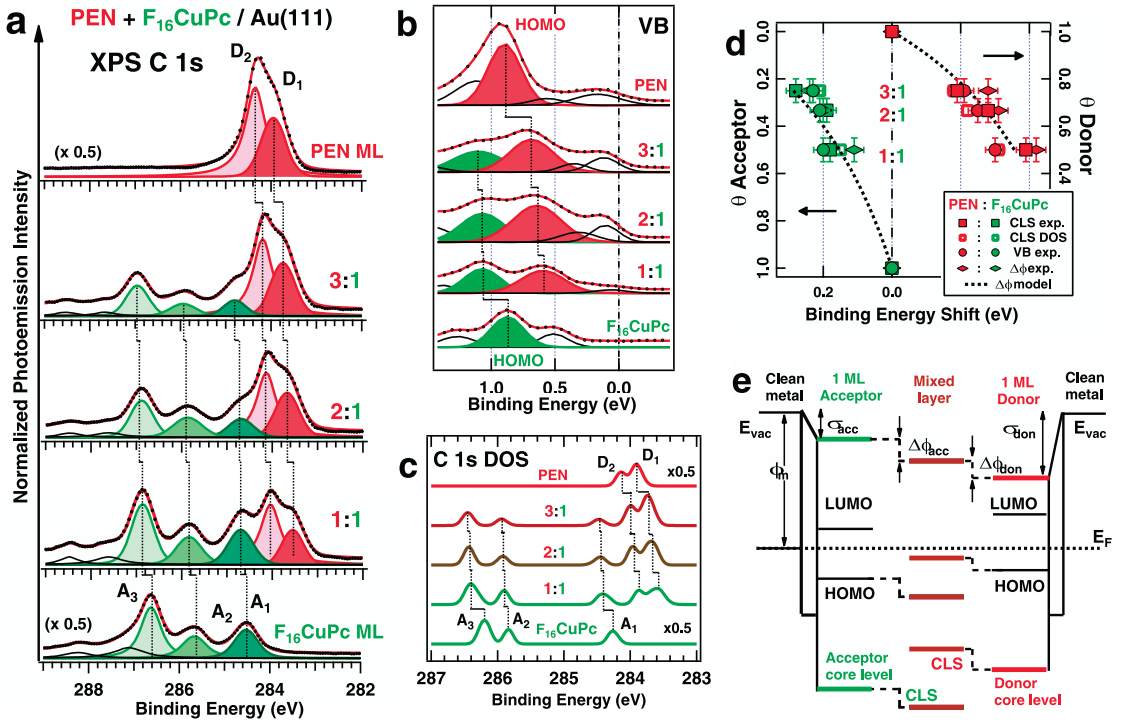

Figure 1. (a) C 1s core-level spectra and (b) valence band spectra from donor-rich (top) to acceptor-rich (bottom) monolayer blends, measured by photoemission on the F_{16}CuPc-PEN/Au(111) system. The assignment of core-level lines to the different atomic species is described in the Methods section. HOMO levels are identified from the comparison with thick film spectra (see Supporting Information Figure S3). Features above the HOMO level and up to E_F vanish in thick films and hence are assumed as interface hybrids.[16] (c) C 1s core levels for F_{16}CuPc-PEN/Au(111) of varying concentration calculated by DFT for free-standing monolayers. (d) Calculated (open squares) and measured (filled squares) A_1 and D_1 core-level shifts for F_{16}CuPc-PEN/Au(111) interfaces. The HOMO peaks and changes in work function for varying stoichiometry are shown by circles and diamonds. The dotted line corresponds to the estimated work function change using pure donor and acceptor layers and eqs 1 and 2 in the text. All core-level, HOMO, and vacuum-level shifts take the reference (zero shift) from pure donor or acceptor layers and show comparable results. (e) Schematic diagram of the energy-level alignment of single-component layers and donor–acceptor blends on metal surfaces. The varying vacuum level and the associated shift of molecular levels upon donor–acceptor blend formation in a vacuum-level pinning scenario are highlighted by dotted lines.

composition of the layer.[13] Under these circumstances, vacuum-level pinning would lead to an effective shift of the Fermi level inside the HOMO–LUMO gap and hence to a variable charge carrier injection/extraction barrier. These barriers, however, are often hard to determine from valence band photoemission spectra in complex multicomponent, molecular/metal systems.[14] We demonstrate that core-level photoemission from donor–acceptor/metal interfaces can straightforwardly and transparently assess interfacial energy-level alignment.

Here, we study systematically varied donor–acceptor molecular networks on metal surfaces. These include blends of perfluorinated copper phthalocyanine (F_{16}CuPc, acceptor) with pentacene (PEN, donor) and the combination of isomorphic molecules with inversed donor/accector character, that is, perfluoropentacene (PFP, acceptor) with copper phthalocyanine (CuPc, donor). In a first step, we deposit donor–acceptor monolayer blends of varying stoichiometry on Au(111), Ag(111), and Cu(111) crystal surfaces held at 300 K. In this context, we made the specific choice of a Cu-metalated phthalocyanine in order to minimize local rehybridization of the organo-metal 3d states with the substrate charge density and have molecule–substrate interactions mainly mediated by molecular ligand π-states.[15] Subsequently, we analyze the electronic properties of those blends exhibiting crystalline order, as determined by scanning tunneling microscopy (Supporting Information Figures S1 and S2). We show that the generic core-level shift that is observed as a function of the donor–acceptor ratio can be directly correlated to the interfacial energy-level alignment regardless of the particular molecules and substrate.

RESULTS AND DISCUSSION

High-resolution C 1s core-level X-ray photoemission (XPS) and valence band (VB) spectroscopy measurements are depicted in Figure 1a and 1b as a function of the donor/acceptor ratio of all observed crystalline structures at the PEN-F_{16}CuPc/Au(111) interface. We immediately notice the relative simplicity of the XPS spectra (Figure 1a) *versus* the difficulties that arise in the interpretation of the valence band of mixed layers

(Figure 1b). In XPS, core-level lines from the different atomic species and molecules can be readily assigned, in contrast to VB spectra, where contributions from both PEN and F_{16}CuPc molecular levels largely overlap. From comparison with thick film spectra (Figure S3) we learn that the strongest VB peak for each molecule corresponds to the HOMO level, while additional emission from interface hybrids (vanishing in thicker films) is observed closer to the Fermi level E_F.[16] In addition to the spectrum's complexity, the low-energy onset, which marks the true hole injection barrier,[17] cannot be defined and tracked as accurately as core levels.

A rightwards (to lower binding energy [BE]) shift is clearly observed in the core levels of Figure 1a, as the concentration of donor molecules decreases from pure donor layers (top), through donor−acceptor blends, to pure acceptor layers (bottom). The same trend is detected for the valence band peaks, particularly HOMO levels in VB photoemission spectra (Figure 1b), and the same is also inferred for LUMO levels from near edge X-ray absorption spectroscopy (NEXAFS) analysis of the same system, as presented in Figure S4. These results suggest a rigid donor−acceptor band structure that shifts as a function of the blend stoichiometry. Note that the rigidity of the molecular electronic band structure allows charge injection/extraction barriers to be followed through core-level shifts. Such core-level tracking analysis has been historically applied to the Schottky barrier problem at inorganic metal/semiconductor interfaces,[18] where the band gap edge is, as in the present case, difficult to define in valence band spectra.

The donor−acceptor core-level shift is both qualitatively and quantitatively reproduced by all-electron DFT calculations within the local density approximation (LDA) of gas-phase, free-standing F_{16}CuPc-PEN mixed layers, as shown in Figure 1c. In Figure 1d, we compare measured core-level and HOMO shifts with the calculated binding energy shift for both F_{16}CuPc and PEN core levels. There is an excellent match between experimental shifts and the free-standing layer calculation. This demonstrates that, despite the presence of interface hybrids, F_{16}CuPc and PEN interact weakly with the Au(111) substrate, and that this weak molecule/surface interaction, typically involving mostly molecular π orbitals and substrate d levels, is not significantly altered upon blending.

To understand the nature of the core-level shift, we may first consider intermolecular charge transfer. The Bader analysis of the charge distribution in the 1:1, 1:2, and 1:3 F_{16}CuPc-PEN free-standing blend indicates significant electronic coupling in spite of the side-by-side donor−acceptor geometry, leading to a net transfer of $\sim$0.3 e^- from the set of one, two, or three donor molecules to the acceptor molecule. The intermolecular electronic coupling is presumably enhanced by the numerous hydrogen bonds present in the blends, which have previously been shown to provide electronic coupling even surpassing that of interfaces composed entirely by C−C σ bonds.[19] Further evidence of intermolecular hybridization is shown in Figure S5, depicting how the PEN HOMO level hybridizes with the levels of F atoms of neighboring F_{16}CuPc molecules.

While "oxidation" ("reduction") of donor (acceptor) molecules shifts core levels to higher (lower) binding energy, our observed shifts follow the opposite direction. In reality, as shown in previous theoretical work on free-standing PFP-CuPc blends,[20] the oxidation−reduction effect in the core levels due to the donor-to-acceptor charge transfer exists and follows the argument above. However, in addition to the charge state of the atoms, core-level energies are known to be determined also by the effect of screening of the atom by the external environment. In the absence of major chemical interactions, the screening can be estimated by the effective potential created by the external environment at the atomic position, and core-level shifts can be reproduced by an additively separable function of charge transfer and change in external potential.[20] Comparing single-component layers and blends, the potential from the substrate remains virtually unchanged and can be neglected, allowing comparison of free-standing molecular layers. Donors create a more binding potential than acceptors, shifting acceptor core levels to higher binding energies as their environment includes more donors and *vice versa*. By way of example, the effective potential comparing pure F_{16}CuPc layers with F_{16}CuPc:PEN blends in a 1:3 ratio changes by −0.34 and −0.25 eV on the F_{16}CuPc benzene C−C and Cu atoms, respectively. The core-level shift for the benzene C−C component calculated by all-electron DFT and shown in Figure 1c amounts to −0.21 eV, and the difference can be ascribed to the contribution of the transferred charge, distributed over the molecule. That is, minor oxidation/reduction effects are compensated and even reversed by the effective potential, which correlates with the molecular ionization potential (IP). In turn, the IP of free-standing layers is analogous to the work function ϕ of the molecular layer/substrate system.

We have measured the work function for each different layer and included the variations, referred to that of pure donor or acceptor monolayers, in Figure 1d. The match between the shifts of core levels (whether measured or calculated) and work function changes as a function of varying stoichiometry is excellent. Such good matching supports the ideal interfacial vacuum-level pinning scenario depicted in Figure 1e, where changes in the vacuum level rigidly shift all molecular levels by the same amount. Under these circumstances, core-level shifts are directly associated with the variation of the charge carrier injection/extraction barriers, which in turn can be directly

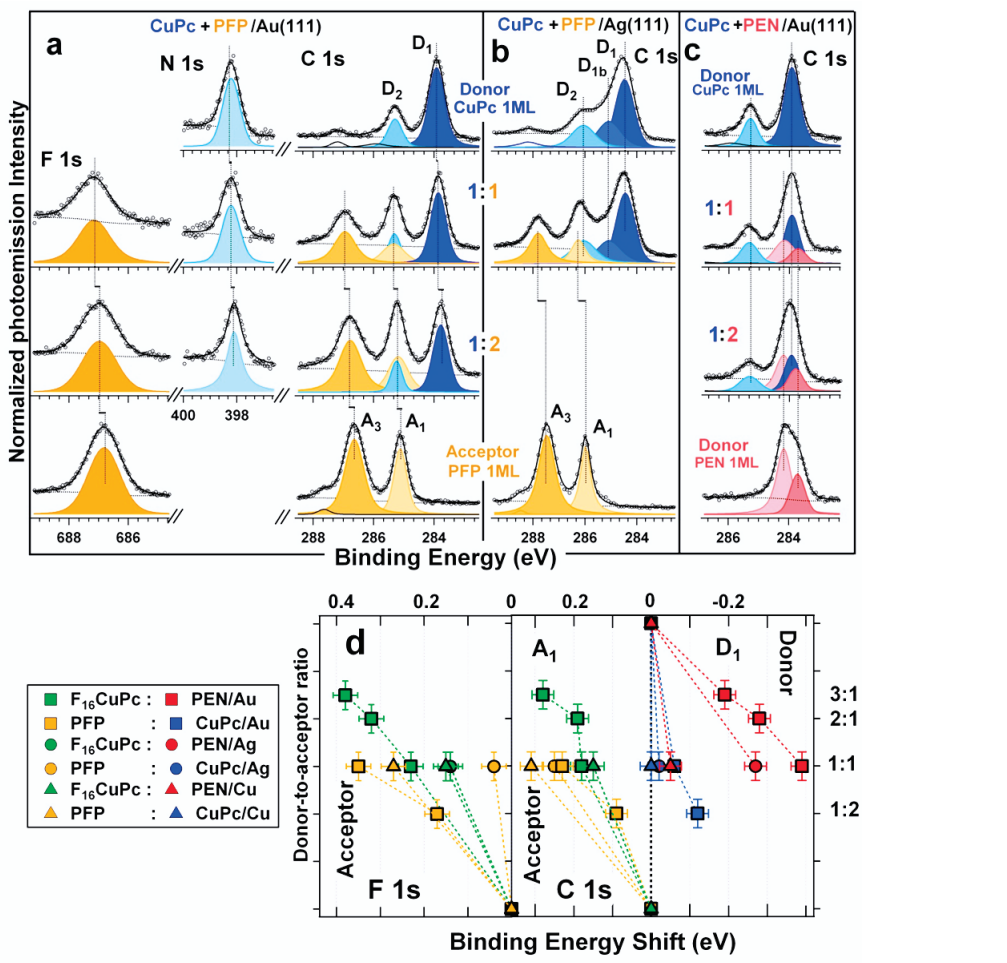

Figure 2. Core levels for monolayer crystal phases of PFP-CuPc on (a) Au(111) and (b) Ag(111), exhibiting the rightward donor-to-acceptor core-level shift. By contrast, in the donor−donor CuPc-PEN/Au(111) blend in (c), core levels show no shift. (d) Summary of F 1s and C 1s core-level shift data in all donor−acceptor/metal interfaces. We represent the lower binding energy component of C 1s for donors (D_1), which is less affected by the overlap with other components, while for acceptors, we choose F 1s and the C−C satellite of the C 1s spectra (A_1). All systems exhibit the same trend, namely, a shift to lower binding energy as we move from donor-rich to acceptor-rich interfaces.

inferred from work function variations $\Delta\phi$. Assuming a linear dependence of the interface dipole with the partial coverage of each molecule,[21] $\Delta\phi$ can be estimated from work function measurements of pure donor and acceptor layers as

$$\Delta\phi_{acc} = \frac{S_{don}}{S_{don} + S_{acc}}(\sigma_{don} - \sigma_{acc}) \quad (1)$$

$$\Delta\phi_{don} = \frac{S_{acc}}{S_{don} + S_{acc}}(\sigma_{acc} - \sigma_{don}) \quad (2)$$

where S_{don} and S_{acc} are the surface area covered by the different molecules, and σ_{don} and σ_{acc} are the interface dipoles associated with pure donor and acceptor monolayers, respectively (Figure 1e). Application of this simple model to the F_{16}CuPc-PEN/Au(111) system results in the dotted line included in Figure 1d. The excellent agreement with the experimentally measured shifts in each of the molecular blends highlights the predictive power of this model using only data of single-component layers, available for a great number of metal−organic systems in the literature.[17,22,23] However, it is important to remember that vacuum-level pinning occurs only for weakly interacting molecule/substrate systems as the case described above. Here, the induced density of interface states (IDIS) within the F_{16}CuPc HOMO−LUMO gap is still away from the Fermi level, providing an interfacial energy-level alignment scenario similar to that in the absence of gap states. On the other hand, the IDIS within the PEN HOMO−LUMO gap is low enough to cause only minor deviations from the vacuum-level pinning scenario. As shown next, deviations from this model increase for increasingly strong molecule/substrate interactions.

Thus, we examine how general these findings are. Figure 2a depicts all core levels resulting from a swapped donor−acceptor character of the molecules by combining PFP and CuPc, and in Figure 2b, the substrate is changed to Ag(111). The behavior is the

same as in Figure 1 in all N, C, and F 1s core levels; that is, we observe an overall shift to lower binding energies from the top spectra, the donor-like molecule/metal interface, to the bottom one, the acceptor-like system. As discussed before, the sign of the shift is at odds with the charge flow direction from donors to acceptors. However, it is in agreement with work function variations since a characteristic property of donor/metal and acceptor/metal interfaces is their different work function, which is generally lower for donor than acceptor monolayers. The Pauli repulsion is larger for the donors CuPc and PEN, as they lie closer to the surface than $F_{16}CuP_C$ and PFP (Figure S1).[23−28] Regarding molecular polarization, fluorinated molecules on strongly interactive metals such as Cu have fluorine atoms located above the C backbone, thereby creating a dipole moment directed toward the surface.[23,24] Besides, donors are expected to donate more charge to the substrate. All of the above explain the lower value of the work function for donor monolayers compared to acceptors and thereby the core-level shifts in a scenario of stoichiometry-dependent work function and weakly interacting molecule/substrate interfaces. In Figure 2c, we level the donor character of the pair by mixing PEN and CuPc. The obtained shift is negligible in all core levels, as expected from the comparable ionization potential of the molecules.[9] Figure 2d summarizes the shifts obtained for the full variety of donor−acceptor interfaces. In all cases, one can observe the same characteristic, rightwards donor-to-acceptor core-level shift, which does not depend upon the nature of the donor or the acceptor nor the core level or the metal substrate.

The core-level shift trend being universal, Figure 2d shows that its magnitude varies from system to system and between core levels. In general, the shift of donors appears to be smaller than that affecting acceptors, being smallest for CuPc donors and for Cu(111) interfaces. The quantitative differences are better observed in Figure 3, where we represent core-level shifts only for 1:1 mixtures on the three substrates. These have the advantage of exhibiting the same 2D crystal structure (Figure S1), implying that changes in the electronic properties of molecular blends from substrate to substrate can be directly ascribed to different molecule−substrate interactions as opposed to intermolecular effects. In the $F_{16}CuPc$-PEN/Au(111) case, we add the vacuum-level shift, which falls close to the calculated core-level shift within 0.1 eV, proving their intimate connection, as discussed before. For acceptors, measured and calculated core-level shifts show a good match, from which we conclude that acceptors, which lie relatively far from the substrate (Figure S1),[23−28] pin their molecular levels to the local vacuum level. In contrast, the core-level shift for donors is reduced with respect to the free-standing film, particularly in CuPc, where it is nearly zero.

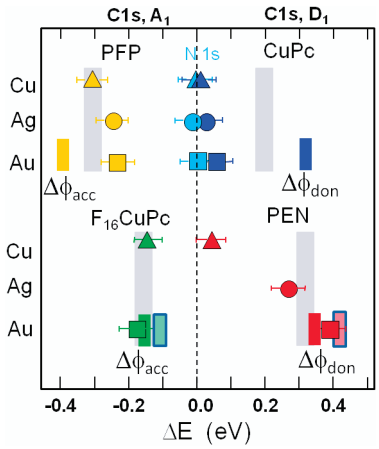

Figure 3. Summarized core-level shifts in 1:1 blends. Data points correspond to the same C 1s core-level shifts of Figure 2. Vertical gray bars mark the corresponding core-level shifts calculated for 1:1 $F_{16}CuPc$-PEN and 1:1 CuPc-PFP free-standing films, the latter presented in ref 20. For the Au(111) interface, we include the vacuum-level shift (small bars). The latter has been either measured (light colored, blue framed) or estimated through eqs 1 and 2 (dark colored) using values of interface dipoles in single-component layers.[17,22] Calculated and measured core-level shifts show good agreement for acceptors, whereas strong deviations are found for donors. Such difference is explained by weak acceptor/metal *versus* strong donor/metal interactions that pin molecular levels to the local vacuum or the Fermi levels, respectively.

We rationalize this by a stronger molecule/metal interaction in donors, which lie closer to the substrate. The proximity induces a larger density of hybrid states inside the HOMO−LUMO gap that pin the molecular orbitals to E_F. A high density of gap states allows the system to accommodate donor−substrate charge transfers without affecting the E_F position significantly.[8,9] In fact, pinning is most apparent in the N 1s core level, as can be understood from the spatial distribution of the CuPc HOMO, which shows higher density of states on the N atoms.[28] Local physical−chemical phenomena such as hybridizations and charge transfer, associated with orbital symmetry and distribution, are therefore held responsible for the differences in the shifts between core levels.

CONCLUSIONS

In conclusion, we observe a rigid connection of core levels and frontier HOMO and LUMO levels in donor−acceptor/metal interfaces, which enables the analysis of charge carrier injection/extraction barrier changes through core-level shift analysis. A characteristic core-level shift in monolayer donor−acceptor blends is observed as a function of the donor/acceptor ratio, which follows the stoichiometry-dependent work function variation according to a local vacuum-level pinning scenario. Deviations thereof, reflecting Fermi-level pinning rather than vacuum-level pinning, affect mostly donors and Cu interfaces and relate to stronger molecule−substrate interactions. With this work, we

do not only advance in the understanding but provide a handle for the control of charge injection barriers in technologically relevant donor−acceptor/metal interfaces.

METHODS

The Au(111), Ag(111), and Cu(111) surfaces were prepared by standard sputtering and annealing cycles, and their cleanliness checked by XPS or STM prior to molecular deposition. CuPc, F_{16}CuPc, and PEN were purchased from Sigma-Aldrich, and PFP from Kanto Denka Kogyo. The molecules have been used as received, except F_{16}CuPc, which was additionally purified by gradient sublimation. Deposition took place from resistively heated Knudsen cells at temperatures around 380 and 190 °C for the phthalocyanines and acenes, respectively, onto single-crystal surfaces held at room temperature. Careful thickness calibration was achieved by use of a calibrated quartz crystal microbalance and corroborated by detailed analysis of the relative core-level peak intensities.

The XPS experiments were performed at the ALOISA beamline of the Elettra synchrotron in Trieste.[29] The XPS data were collected by means of a hemispherical electron energy analyzer characterized by a ±1° angular resolution, with a photon energy of 140 eV (valence band), 530 eV (C 1s, N 1s), and 810 eV (F 1s). The binding energy of core-level spectra is carefully calibrated taking the substrate core-level energies as absolute references. The fitting of all XPS spectra was done using a Shirley background and Voigt integral functions. Due to the high complexity of the C 1s spectra of the blends, the Lorentzian width, fwhm, and intensity ratio among the different components of the same species are inferred from the analysis of the pure monolayer spectra and kept almost fixed across the mixed phase spectra series, while BEs are left as free parameters of the fit. In the C 1s spectrum of a F_{16}CuPc ML (bottom part of Figures 1 and 2d), three core-level states are clearly observed. The assignment of the different core-level lines is based on previous findings[22,30−32] in which the components deriving from benzene C−C (A_1), pyrrole C−N (A_2), and benzene C−F (A_3) are singled out. The fitted intensity ratios for the different carbon peaks agree well with the expected (2:2:4) C−C, C−N, C−F ratio for this molecule. In the case of the PEN monolayer, the deconvolution of the C 1s spectra into two components (D_1 and D_2 in Figures 1a and 2c, whose main contribution corresponds to the C atoms bonded to H atoms for the former or solely to C for the latter) leads to an excellent fit. While a more rigorous four-component model supported by theoretical calculations[33] and corroborated in a number of studies[7,34] could have provided a satisfactory fit as well, we have opted for a lesser number of peaks in order to simplify the analysis of the mixed phase spectra. The C 1s spectrum of PFP (Figure 2) displays two components that originate from the 8 C atoms bound to neighboring C atoms (A_1) and to the 14 C atoms directly bound to F (A_3), as previously suggested for XPS spectra of PFP on Cu(111) and Au(111).[23,32] Finally, when CuPc is deposited on Au(111), the C 1s spectrum is well reproduced by two peaks, one arising from the carbon atoms bound to H, together with those bound solely to C (labeled D_1 in Figure 2a) and another from C atoms with bonds to N (D_2). On the other hand, an additional component is required when CuPc is deposited on Ag(111) (labeled D_{1b} in Figure 2b), attributed to the C atoms bound solely to C atoms, now differentiated from those with C−H bonds.

Valence band spectra were taken at a photon energy of 140 eV with an overall energy resolution of 200 meV. The surface was oriented with both the electric field incidence and the emission direction (detector orientation) at the magic angle (∼55°). The spectra were aligned at Fermi level and normalized to the photon flux. For the fitting analysis, the clean gold VB spectrum was previously subtracted. The fit procedure of all the VB spectra was then made using a Shirley background and Voigt integral functions. The work function was determined by measuring the variation of the low-energy electron's cutoff (sample bias of −35.00 V), the Fermi edge, and the corresponding absolute photon energy (from the difference between the Au 4f peak measured at the first and second diffraction order of the monochromator at a first order photon energy of ∼180 eV). All the $\Delta\phi$ measurements are referred to the low-energy cutoff of the freshly prepared Au(111) surface. After each cleaning cycle, the work function of the Au(111), ϕ_m, varied between 5.48 and 5.56 eV.

STM measurements were performed at room temperature in commercial Omicron VT-STM and JEOL STM systems in constant current mode. Subsequent analysis of the STM images has been performed with the freeware WSxM from Nanotec Electronica S.L.[35]

The details of the theoretical procedure used in Figure 2 have been published elsewhere.[20] We use the lattice parameters of the corresponding F_{16}CuPc-PEN phases as determined by STM. Core-level energies are obtained using an all-electron calculation within the projector augmented wave function methodology using the local density approximation. The overall accuracy is ±50 meV.

Conflict of Interest: The authors declare no competing financial interest.

Acknowledgment. This work was supported by the Spanish MICINN (MAT2010-21156-C03-01 and -C03-03), the Basque Government (IT-621-13 and -578-13), European Research Council Advanced Grant DYNamo (ERC-2010-AdG Proposal No. 267374), and Spanish Grants FIS2010-21282-C02-01 and PIB2010US-00652. J.L.C. acknowledges financial support from the Mexican CONACyT program, D.J.M. from the Spanish "Juan de la Cierva" program (JCI-2010-08156), and D.G.O. from the European Union under FP7-PEOPLE-2010-IOF-271909.

Supporting Information Available: Data on crystalline structure of molecular blends (Figures S1 and S2), HOMO and LUMO level alignment (Figures S3 and S4),and intermolecular charge transfer (Figure S5). This material is available free of charge *via* the Internet at http://pubs.acs.org.

REFERENCES AND NOTES

1. Horowitz, G. Organic Thin Film Transistors: From Theory to Real Devices. *J. Mater. Res.* **2004**, *19*, 1946–1962.
2. Brutting, W. *Physics of Organic Semiconductors*; Wiley: Weinheim, Germany, 2005.
3. Klauk, H. *Organic Electronics: Materials, Manufacturing and Applications*; Wiley: Weinheim, Germany, 2006.
4. Wakayama, Y.; de Oteyza, D. G.; Garcia-Lastra, J. M.; Mowbray, D. J. Solid-State Reactions in Binary Molecular Assemblies of F_{16}CuPc and Pentacene. *ACS Nano* **2011**, *5*, 581–589.
5. de Oteyza, D. G.; Garcia-Lastra, J. M.; Corso, M.; Doyle, B. P.; Floreano, L.; Morgante, A.; Wakayama, Y.; Rubio, A.; Ortega, J. E. Customized Electronic Coupling in Self-Assembled Donor−Acceptor Nanostructures. *Adv. Funct. Mater.* **2009**, *19*, 3567–3573.
6. de Oteyza, D. G.; Silanes, I.; Ruiz-Oses, M.; Barrena, E.; Doyle, B. P.; Arnau, A.; Dosch, H.; Wakayama, Y.; Ortega, J. E. Balancing Intermolecular and Molecule−Substrate Interactions in Supramolecular Assemblies. *Adv. Funct. Mater.* **2009**, *19*, 259–264.
7. El-Sayed, A.; Mowbray, D. J.; Garcia-Lastra, J. M.; Rogero, C.; Goiri, E.; Borghetti, P.; Turak, A.; Doyle, B. D.; Dell'Angela, M.; Floreano, L.; *et al.* Supramolecular Environment-Dependent Electronic Properties of Metal−Organic Interfaces. *J. Phys. Chem. C* **2012**, *116*, 4780–4785.
8. Betti, M. G.; Kanjilal, A.; Mariani, C.; Vazquez, H.; Dappe, Y. J.; Ortega, J.; Flores, F. Barrier Formation at Organic Interfaces in a Cu(100)-Benzenethiolate-Pentacene Heterostructure. *Phys. Rev. Lett.* **2008**, *100*, 027601.

9. Hwang, J.; Wan, A.; Kahn, A. Energetics of Metal–Organic Interfaces: New Experiments and Assessment of the Field. *Mater. Sci. Eng., R* **2009**, *64*, 1–31.
10. Hill, I. G.; Rajagopal, A.; Kahn, A.; Hu, Y. Molecular Level Alignment at Organic Semiconductor–Metal Interfaces. *Appl. Phys. Lett.* **1998**, *73*, 662.
11. Zou, Y.; Kilian, L.; Scholl, A.; Schmidt, Th.; Fink, R.; Umbach, E. Chemical Bonding of PTCDA on Ag Surfaces and the Formation of Interface States. *Surf. Sci.* **2006**, *600*, 1240–1251.
12. Wandelt, K.; Markert, K.; Dole, P.; Jablonskit, A.; Niemantsverdriett, J. W. Surface Characterization by Means of Photoemission of Adsorbed Xenon (PAX). *Surf. Interface Anal.* **1988**, *12*, 15.
13. Opitz, A.; Bronner, M.; Brutting, W.; Himmerlich, M.; Schaefer, J. A.; Krischok, S. Electronic Properties of Organic Semiconductor Blends: Ambipolar Mixtures of Phthalocyanine and Fullerene. *Appl. Phys. Lett.* **2007**, *90*, 212112.
14. Aygu, U.; Hintz, H.; Egelhaaf, H.-J.; Distler, A.; Abb, S.; Peisert, H.; Chasse, T. Energy Level Alignment of a P3HT/Fullerene Blend During the Initial Steps of Degradation. *J. Phys. Chem. C* **2013**, *117*, 4992–4998.
15. Grobosch, M.; Aristov, V. Y.; Molodtsova, O. V.; Doyle, B. D.; Nannarone, S.; Knupfer, M. Engineering of the Energy Level Alignment at Organic Semiconductor Interfaces by Intramolecular Degrees of Freedom: Transition Metal Phthalocyanines. *J. Phys. Chem. C* **2009**, *113*, 13219–13222.
16. Duhm, S.; Gerlach, A.; Salzmann, I.; Broker, B.; Hohnson, R. L.; Schreiber, F.; Koch, N. PTCDA on Au(111), Ag(111) and Cu(111): Correlation of Interface Charge Transfer to Bonding Distance. *Org. Electron.* **2008**, *9*, 111–118.
17. Koch, N.; Vollmer, A.; Duhm, S.; Sakamoto, Y.; Suzuki, T. The Effect of Fluorination on Pentacene/Gold Interface Energetics and Charge Reorganization Energy. *Adv. Mater.* **2007**, *19*, 112–116.
18. Monch, W. On the Physics of Metal-Semiconductor Interfaces. *Rep. Prog. Phys.* **1990**, *53*, 221–278.
19. de Rege, P. J. F.; Williams, S. A.; Therien, M. J. Direct Evaluation of Electronic Coupling Mediated by Hydrogen Bonds: Implications for Biological Electron Transfer. *Science* **1995**, *269*, 1409–1413.
20. Cabellos, J. L.; Mowbray, D. J.; Goiri, E.; El-Sayed, A.; Floreano, L.; de Oteyza, D. G.; Rogero, C.; Ortega, J. E.; Rubio, A. Understanding Charge Transfer in Donor–Acceptor/Metal Systems: A Combined Theoretical and Experimental Study. *J. Phys. Chem. C* **2012**, *116*, 17991–18001.
21. Fukagawa, H.; Yamane, H.; Kera, S.; Okudaira, K. K.; Ueno, N. Experimental Estimation of the Electric Dipole Moment and Polarizability of Titanyl Phthalocyanine Using Ultraviolet Photoelectron Spectroscopy. *Phys. Rev. B* **2006**, *73*, 041302.
22. Peisert, H.; Knupfer, M.; Schwieger, T.; Fuentes, G. G.; Olligs, D.; Fink, J.; Schmidt, Th. Fluorination of Copper Phthalocyanines: Electronic Structure and Interface Properties. *J. Appl. Phys.* **2003**, *93*, 9683–9692.
23. Koch, N.; Gerlach, A.; Duhm, S.; Glowatzki, H.; Heimel, G.; Vollmer, A.; Sakamoto, Y.; Suzuki, T.; Zegenhagen, J.; Rabe, J. P.; *et al.* Adsorption-Induced Intramolecular Dipole: Correlating Molecular Conformation and Interface Electronic Structure. *J. Am. Chem. Soc.* **2008**, *130*, 7300–7304.
24. Gerlach, A.; Schreiber, F.; Sellner, S.; Dosch, H.; Vartanyants, I. A.; Cowie, B. C. C.; Lee, T.-L.; Zegenhagen, J. Adsorption-Induced Distortion of $F_{16}CuPc$ on Cu(111) and Ag(111): An X-ray Standing Wave Study. *Phys. Rev. B* **2005**, *71*, 205425.
25. Duhm, S.; Hosoumi, S.; Salzmann, I.; Gerlach, A.; Oehzelt, M.; Wedl, B.; Lee, T.-L.; Schreiber, F.; Koch, N.; Ueno, N.; *et al.* Influence of Intramolecular Polar Bonds on Interface Energetics in Perfluoro-Pentacene on Ag(111). *Phys. Rev. B* **2010**, *81*, 045418.
26. Kroger, I.; Stadtmuller, B.; Kleimann, C.; Rajput, P.; Kumpf, C. Normal-Incidence X-ray Standing-Wave Study of Copper Phthalocyanine Submonolayers on Cu(111) and Au(111). *Phys. Rev. B* **2011**, *83*, 195414.
27. Kroger, I.; Stadtmuller, B.; Stadler, C.; Ziroff, J.; Kochler, M.; Stahl, A.; Pollinger, F.; Lee, T.-L.; Zegenhagen, J.; Reinert, F.; *et al.* Submonolayer Growth of Copper-Phthalocyanine on Ag(111). *New J. Phys.* **2010**, *12*, 083038.
28. de Oteyza, D. G.; El-Sayed, A.; Garcia-Lastra, J. M.; Goiri, E.; Krauss, T. N.; Turak, A.; Barrena, E.; Dosch, H.; Zegenhagen, J.; Rubio, A.; *et al.* Copper-Phthalocyanine Based Metal–Organic Interfaces: The Effect of Fluorination, the Substrate, and Its Symmetry. *J. Chem. Phys.* **2010**, *133*, 214703.
29. Floreano, L.; Cossaro, A.; Gotter, R.; Verdini, A.; Bavdek, G.; Evangelista, F.; Ruocco, A.; Morgante, A.; Cvetko, D. Periodic Arrays of Cu-Phthalocyanine Chains on Au(110). *J. Phys. Chem. C* **2008**, *112*, 10794–10802.
30. Biswas, I.; Peisert, H.; Nagel, M.; Casu, M. B.; Schuppler, S.; Nagel, P.; Pellegrin, E.; Chasse, T. Buried Interfacial Layer of Highly Oriented Molecules in Copper Phthalocyanine Thin Flms on Polycrystalline Gold. *J. Chem. Phys.* **2007**, *126*, 174704.
31. Piper, L. F. J.; Cho, S. W.; Zhang, Y.; DeMasi, A.; Smith, K. E.; Matsuura, A. Y.; McGuinness, C. Soft X-ray Spectroscopy Study of the Element and Orbital Contributions to the Electronic Structure of Copper Hexadecafluoro-Phthalocyanine. *Phys. Rev. B* **2010**, *81*, 045201.
32. de Oteyza, D. G.; Sakko, A.; El-Sayed, A.; Goiri, E.; Floreano, L.; Cossaro, A.; Garcia-Lastra, J. M.; Rubio, A.; Ortega, J. E. Inversed Linear Dichroism in F K-Edge NEXAFS Spectra of Fluorinated Planar Aromatic Molecules. *Phys. Rev. B* **2012**, *86*, 075469.
33. Baldacchini, C.; Allegretti, F.; Gunnella, R.; Betti, M. G. Molecule–Metal Interaction of Pentacene on Copper Vicinal Surfaces. *Surf. Sci.* **2007**, *601*, 2603–2606.
34. Ferretti, A.; Baldacchini, C.; Calzolari, A.; Felice, R. D.; Ruini, A.; Molinari, E.; Betti, M. G. Mixing of Electronic States in Pentacene Adsorption on Copper. *Phys. Rev. Lett.* **2007**, *99*, 046802.
35. Horcas, I.; Fernandez, R.; Gomez-Rodriguez, J. M.; Colchero, J.; Gomez-Herrero, J.; Baro, A. M. WSxM: A Software for Scanning Probe Microscopy and a Tool for Nanotechnology. *Rev. Sci. Instrum.* **2007**, *78*, 013705.